Modeling the Free Radical Solution and Bulk Polymerization of Methyl Methacrylate

BRIAN M. LOUIE, GREGORY M. CARRATT, and DAVID S. SOONG,
Department of Chemical Engineering, University of California, Berkeley, California 94720

Synopsis

This paper reviews our current understanding of the kinetics and mechanisms of free-radical chain polymerization of methyl methacrylate. A mathematical model previously proposed to describe the bulk polymerization of MMA is here extended to cover solution polymerization. This extended model is validated by comparing its predictions with experimental data over a range of conversions and product molecular weights.

INTRODUCTION

Methyl methacrylate is often polymerized by a free-radical, chain addition mechanism. This process consists of three steps: initiation, propagation, and termination. Free radicals are formed by the fragmentation of initiators. Once formed, these radicals propagate by reacting with surrounding monomers to form long chains—the active site being shifted to the end of the chain when a new monomer is added. The reaction terminates when two radicals react. Because only trace quantities of radicals exist at a time, propagation occurs much more frequently than termination. The mean lifetime of a radical is on the order of a couple of seconds, but, in that time, several hundred monomers may have reacted with it. Table I summarizes the basic free radical polymerization mechanism.

The kinetics are often complex because the growing and dead polymers reduce chain mobility and hamper radical termination. A strong autoacceleration in the rate first occurs along with a concomitant increase in the medium viscosity. A limiting conversion is later reached when even the propagation step is slowed by the high viscosity. Hence, modeling the kinetics of methyl methacrylate must take these considerations into account. A detailed understanding of each step is needed if accurate predictions are to be achieved.

CHAIN INITIATION

Free radicals are usually produced by the thermal decomposition of an initiator, such as benzoyl peroxide (BPO) or 2,2'-azobisisobutyronitrile (AIBN). Both fragment easily into two primary radicals and a gas molecule. The primary radicals then react with surrounding monomers to initiate growing polymer chains. Fragmentation is the limiting step in the initiation process. Free radicals can also be produced by the photodecomposition of a sensitizer,[1] or by the thermal decomposition of the monomer.[2] However,

Journal of Applied Polymer Science, Vol. 30, 3985–4012 (1985)
 CCC 0021-8995/85/103985-28$04.00

TABLE I
Free-Radical Kinetics of Methyl Methacrylate Polymerization[a]

Initiation:	$I \xrightarrow{k_d} 2\,R\cdot + G\uparrow$	$R_d = k_d[I]$
	$R\cdot + M \xrightarrow{k_i} P_1\cdot$	$R_i = k_i[R\cdot][M]$
	$2\,R\cdot \xrightarrow{k_{ti}} I'$	$R_{ti} = k_{ti}[R\cdot]^2$
Propagation:	$P_n\cdot + M \xrightarrow{k_p} P_{n+1}\cdot$	$R_p = k_p[P_n\cdot][M]$
Termination:	$P_n\cdot + P_m\cdot \xrightarrow[\text{(combination)}]{k_{tc}} D_{n+m}$	$R_{tc} = k_{tc}[P_n\cdot][M]$
	$P_n\cdot + P_m\cdot \xrightarrow[\text{(disproportionation)}]{K_{td}} D_n + D_m$	$R_{td} = k_{td}[P_n\cdot][P_m\cdot]$

[a] Symbols: I = initiator (AIBN), R· = primary radical, I′ = recombined initiator fragments, G = gas molecule (nitrogen), M = monomer (MMA), $P_n\cdot$ = live radical of length n, D_n = dead polymer of length $_n$, k_d = initiator decomposition rate constant, k_i = chain initiation rate constant, k_{ti} = primary radical recombination rate constant, k_p = propagation rate constant, k_{td} = termination by disproportionation rate constant, and k_{tc} = termination by combination rate constant.

Wallings and Briggs[2] found the thermal initiation of MMA almost negligible even at 100°C.

Not all primary radicals produce propagating chains. Once formed, primary radicals execute many oscillations in "cages" consisting of surrounding molecules before they diffuse apart. During this time, the primary radicals may react with one another to form an inactive species. To account for this recombination, an initiator efficiency f is used. Whether the initiator efficiency is a constant or not is a point of controversy. Biesenberger and Sebastian[3] believe that f is a strong function of the monomer conversion, and should decrease throughout the entire course of the reaction. Depletion of monomer increases the difficulty of primary radicals initiating new chains. However, Cardenas and O'Driscoll[4] and Soh and Sundberg[5] argued that f should remain constant until very high conversions because primary radicals are not subject to significant diffusional effects. Primary radicals should have no difficulty finding monomers to initiate new chains. The experimental work of Brooks[6] supported this conclusion. He found the initiator efficiency to remain constant and independent of the viscosity.

Initiation of AIBN in different solvents was investigated by Kulkarni et al.[7] They found solvent played no role in the decomposition of AIBN. Decomposition rates were also found to be independent of the viscosity of the medium. The same conclusion was reached by Arnett[8] and Lewis and Matheson[9]; however, Petersen et al.[10] did find a minor dependence on the solvent used.

CHAIN PROPAGATION AND THE GLASS EFFECT

Once primary radicals are generated, they quickly react with monomer to form long polymer chains. At 70°C and 0.0258M AIBN, well over 1000 monomer molecules can be added to a single chain in 0.25 s. Radical reac-

tivity is usually assumed independent of the chain length of the radical as only the chain end is needed for the reaction. Propagation ends when either the equilibrium monomer concentration (to be defined later) has been reached or a glass is formed. In the glassy state, even the motion of small molecules is severely restricted.[11] This sets a limiting conversion on the polymerization process. Martin and Hamielec[12] found the limiting conversion to decrease almost linearly with decreasing temperature for bulk polymerization of MMA. Balke and Hamielec[13] correlated glass formation with a free volume of the reacting mixture. They found a glass was formed when the free volume fraction dropped below 0.025.

Experimental results from emulsion polymerization suggest that k_p may well be constant until near the end of the polymerization.[14] This is supported by both Ross and Laurence[15] and Martin and Hamielec,[12] who found the onset of the glass effect occurred around a free volume fraction of 0.05 and 0.066, respectively. These free volumes correspond to very high conversions. However, Hayden and Melville[16] measured the absolute propagation rate constant k_p for MMA and found it to fall off around 50% conversion. They reasoned that the propagation step is diffusion-controlled at high conversion. By being diffusion controlled, propagation can only occur as rapidly as the monomer can arrive at the growing end. The drop in k_p is thought to be caused by the high viscosities encountered during the later stages of polymerization.

CHAIN TRANSFER

Not every propagation step leads to lengthening of the radical chain. Transfer of the active site from one macroradical to another molecule is yet another possibility. This radical transfer process terminates the growing radical and initiates a new polymer chain. The process involves abstracting a hydrogen atom from a donor molecule, converting it into a transfer radical. The donor molecule can be (1) the monomer, (2) the polymer, (3) the initiator, or (4) any solvent (see Table II). Any impurities in the reacting medium can also cause chain transfer. Growth of the new chain occurs when the transferred radical reacts with more monomer. Chain transfer reactions are usually ignored in modeling bulk polymerization. However, chain transfer to solvent and monomer may have significant impact for solution polymerization.[17,18] This point is discussed further in a later section.

CHAIN TERMINATION

Termination occurs when two radicals react via a bimolecular process. PMMA produced during the polymerization raises the viscosity of the reacting medium and can affect the mobility of the macroradicals. North and co-workers[19-21] found that the termination rate is diffusion controlled even at zero conversion. They suggest that the average termination rate constant k_t should be proportional to the diffusivity of the radicals.

North proposed that the termination process be divided into three steps. Initially, two radicals are separated in space. The radicals move toward one another by translation of the center of mass of the macroradical chain. Once in close proximity of each other, the active chain ends must orient in the closest neighbor configuration. Only then can the radicals react to

TABLE II
Side and Chain Transfer Reactions of PMMA Polymerization[a]

Negligible side reactions				
Thermal initiation:	M	$\xrightarrow{k_{di}}$	$2R\cdot$	$R_{di} = 2k_{di}[M]^2$
Terminal double bond:	$P_n\cdot + D_m$	$\xrightarrow{k_{pt}}$	$P_{n+m}\cdot$	$R_{pt} = k_{pt}[P_n\cdot][D_m]$
Chain transfer reactions				
With monomer:	$P_n\cdot + M$	$\xrightarrow{k_f}$	$P_1\cdot + D_n$	$R_f = k_f[M][P_n\cdot]$
With polymer:	$P_n\cdot + D_m$	$\xrightarrow{k_{fp}}$	$D_n + P_m\cdot$	$R_{fp} = k_{fp}[D_m][P_n\cdot]$
With solvent:	$P_n\cdot + S$	$\xrightarrow{k_s}$	$D_n + S\cdot$	$R_s = k_s[S][P_n\cdot]$
	$S\cdot + M$	$\longrightarrow$	$S + P_1\cdot$	
With initiator:	$P_n\cdot + I$	$\xrightarrow{k_{fi}}$	$D_n + I\cdot$	$R_{fi} = k_{fi}[I][P_n\cdot]$
	$I\cdot + M$	$\longrightarrow$	$I + P_1\cdot$	

[a] Symbols: $S\cdot$ = solvent transfer radical, $I\cdot$ = initiator transfer radical, k_{di} = thermal initiation rate constant, k_{pt} = terminal double bond rate constant, k_f = chain transfer to monomer rate constant, k_{fp} = chain transfer to polymer rate constant, k_s = chain transfer to solvent rate constant, and k_{fi} = chain transfer to initiator rate constant.

terminate (see Fig. 1). Radicals terminate via two paths. The microradicals can combine to form a single chain (combination) or form two dead chains (disproportionation). Bevington et al.[22] measured the relative rate of disproportionation to combination for MMA at different temperatures. He found that disproportionation dominated at high temperatures ($T > 70$°C), while combination was important at low temperatures ($T < 40$°C).

When termination occurs by disproportionation, a terminal double bond remains. Branching may occur if this double bond is attacked and incorporated into another growing radical (see Table II). This side reaction increases both $\overline{M}_n$ and $\overline{M}_w$ by decreasing the number of polymer chains while increasing the weight of the polymer formed, and is significant for vinyl acetate.[23] However, Morton and Piirma[24] found little or no branching to occur in MMA. This observation may be explained by noting that the double

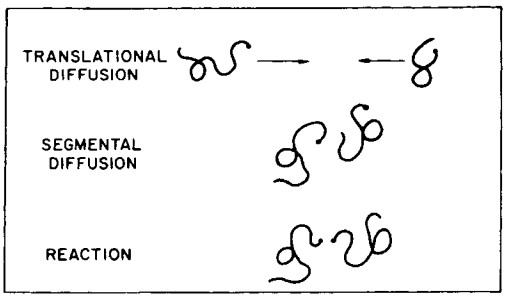

Fig. 1. Diffusion controlled termination occurs in three steps. Radicals first move (translate) into close proximity with one another, align active centers by segmental motion, and then finally react.

bond of monomer molecules have a greater mobility than a terminal double bond attached to a slow moving polymer chain. Thus, growing radicals are more likely to react with monomer than terminal double bonds.

THE GEL EFFECT

A key feature in the polymerization of MMA is the gel effect. The gel effect appears as a sharp increase in the rate of reaction, usually accompanied by an increase in viscosity. Onset of the gel effect occurs between 20 and 40% conversion, depending on the temperature and the amount of initiator used.[25] Numerous investigations have tried to correlate the onset of the gel effect using the form

$$K_c = c\overline{M}_n^a \tag{1}$$

where c is the concentration of polymer, $\overline{M}_n$ represents the number average molecular weight of the polymer, and K_c and a are constants. When $a = ½$, the onset occurs when polymer molecules begin to close pack.[26,27] When $a = 1$, the onset is caused by the formation of an entangled network. Lee and Turner[28-31] found K_c to have a slight temperature dependence in the range from 30 to 90°C and that the polymer concentration is correctly incorporated. However, a wide range of values for a have been reported.[28-36] Others[37,38] have tried to correlate the onset of the gel effect to a critical bulk viscosity. The gel effect can be explained by a decrease in the termination rate.[16] As the termination rate decreases, radical populations increase with accompanying acceleration of polymerization. Much longer polymer molecules are created as the mean lifetime of the macroradicals is lengthened.

Trommsdroff et al.,[39] Norrish and Smith,[40] and Schultz and Harborth[41] believed that high viscosity causes the decrease in the termination rate. Trommsdroff added premade PMMA to the monomer to induce a gel effect, while Schultz and Harborth added a solvent to eliminate it. But Benson and North[20] investigated the effect of solvent viscosity on the termination and found the termination rate constant to be inversely proportional to the solution viscosity at low conversion. This relationship overestimates the decrease in termination rate for bulk polymerization of MMA[6,19] when MMA is used as the solvent for PMMA. Hence, viscosity alone cannot account for the gel effect.

DERIVATION OF MODEL EQUATIONS

In order to improve existing processes and devise new ones, an in-depth, concise understanding of the underlying chemical phenomena is needed. The next step is to construct a mathematical model incorporating these phenomena and aforementioned diffusion considerations to predict the polymerization behavior of methyl methacrylate. Model building consists of several distinct phases.

The first step is to identify the kinetic mechanism. The important equations are shown in Tables I and II. All significant macroradical reactions are listed. Chain initiation, propagation, and termination are the major ones to the reaction scheme. Radical transfer to solvent and to monomer

is considered for accurate molecular weight predictions. But, branching reactions, thermal initiation of monomer, and all other transfer reactions can be ignored, as previously discussed.

The second step is to develop the species mass balance equations from the kinetic scheme. This leads to the set of equations shown in Table III. Monomer consumption by primary radicals and chain transfer reactions has been ignored (long chain hypothesis). This is usually valid when the kinetic chain length is long. The rate of initiation is simplified by incorporating primary radical termination with an initiator efficiency factor:

$$2fk_d[\mathrm{I}] = 2k_d[\mathrm{I}] - k_{ti}[\mathrm{R}]^2 \tag{2}$$

The quasi-steady-state approximation (QSSA) is applied to primary radicals only. The QSSA is not extended to calculation of the macroradical population, as the approximation breaks down at high conversions. Chiu et al.[42] showed that the approximation can lead to a 10% error. Thus, all radical equations remain in differential form.

The next step is to simplify the infinite number of radical population equations into a smaller set of modeling equations. This can be done by using moments. Moments are defined by

$$\lambda_k = \sum_{n=1}^{\infty} n^k[\mathrm{P}_n] \tag{3}$$

$$\mu_k = \sum_{n=1}^{\infty} n^k[\mathrm{D}_n] \tag{4}$$

where λ_k and μ_k are the kth moments of the live and dead polymer chains respectively. Note that $[\lambda_0]$ is the total radical concentration, and $[\mu_0]$ is the total concentration of dead polymer, while $[\lambda_1] + [\mu_1]$ is the number of moles of monomer which has reacted.

TABLE III
Species Balance Equations for a Batch Reactor

$\frac{1}{V}\frac{d([\mathrm{M}]V)}{dt} = -k_p[\mathrm{M}]\lambda_0$	(1)
$\frac{1}{V}\frac{d([\mathrm{I}]V)}{dt} = -k_d[\mathrm{I}]$	(2)
$\frac{1}{V}\frac{d([\mathrm{R}\cdot]V)}{dt} = 2fk_d[\mathrm{I}] - k_t[\mathrm{R}\cdot][\mathrm{M}] = 0$	(3)
$\frac{1}{V}\frac{d([\mathrm{S}]V)}{dt} = 0$	(4)
$\frac{1}{V}\frac{d([\mathrm{P}_1\cdot]V)}{dt} = 2fk_d[\mathrm{I}] - k_t[\mathrm{P}_1\cdot]\lambda_0 + k_f[\mathrm{M}]\lambda_0 + k_s[\mathrm{S}]\lambda_0$	(5)
$\frac{1}{V}\frac{d([\mathrm{P}_n\cdot]V)}{dt} = k_p[\mathrm{M}]([\mathrm{P}_{n-1}\cdot] - [\mathrm{P}_n\cdot]) - k_t[\mathrm{P}_n\cdot]\lambda_0 - k_f[\mathrm{M}][\mathrm{P}_n\cdot] - k_s[\mathrm{S}][\mathrm{P}_n\cdot] \quad \text{for } n \geq 2$	(6)
$\frac{1}{V}\frac{d([\mathrm{D}_n]V)}{dt} = k_{td}[\mathrm{P}_n\cdot]\lambda_0 + \frac{1}{2}k_{tc}\sum_{m=1}^{n-1}[\mathrm{P}_{n-m}\cdot][\mathrm{P}_m\cdot] + k_f[\mathrm{M}][\mathrm{P}_n\cdot] + k_s[\mathrm{S}][\mathrm{P}_n\cdot] \quad \text{for } n \geq 1$	(7)

Volume contraction (a reduction of ~30% at complete conversion) is significant during the reaction and must be incorporated. The volume contraction factor is

$$\epsilon = (\rho_p - \rho_m)/\rho_p \tag{5}$$

where the density of the polymer, ρ_p, is appreciably greater than the density of monomer, ρ_m. The addition of a solvent does not affect the basic assumption of linear volume dependence on conversion. Assuming additivity of volumes (or equivalently no volume change on mixing), we have

$$V = V_m + V_p + V_s \tag{6}$$

where V_s is the volume of solvent and V is the volume of the mixture. Volume of the monomer, V_m, and volume of the polymer, V_p, can be related to the initial charge of monomer, M_0, and conversion x in the batch:

$$V = \frac{M_0(1 - x)}{\rho_m} + \frac{M_0 x}{\rho_p} + \frac{M_s}{\rho_s} \tag{7}$$

The mass of solvent, M_s, can be related to the volume fraction of solvent, f_s, in the batch. Equation (7) then becomes

$$V = V_m^0 (1 - \epsilon x + \beta) \tag{8}$$

where β is $f_s/(1 - f_s)$ and V_m^0 is the initial volume of monomer. The initial volume of monomer can then be linked to the initial volume, V_0, by

$$V_m = V_0 (1 - f_s) = V_0/(1 + \beta) \tag{9}$$

The fractional conversion is defined as

$$x = ([\mathrm{M}]_0 V_0 - [\mathrm{M}] V)/[\mathrm{M}]_0 V_0 \tag{10}$$

where [M] is the concentration of monomer and $[\mathrm{M}]_0$ is that of pure monomer. The above definitions are then substituted into the species balances (Table III) to give a set of ordinary differential equations for modeling a batch polymerization (Table IV).

Since there are more unknowns than equations, a set of constitutive equations or relations must be developed to make the model tractable. A set of these equations for the physical properties of the monomer, polymer, and solvent along with most of the rate constants is presented in Table V. The heart of the kinetic model, the constitutive equations used for the gel and glass effects, will be derived in the next section. A review of other existing gel and glass effect equations is given in Ref. 52.

THE CCS MODEL

Modeling of the gel effect must entail a firm understanding of the diffusion processes of radical species in a polymeric matrix. North and Reed[19] found that the initial termination rate is segmental diffusion-controlled.

TABLE IV
Rate Equations for an Isothermal Batch Reactor

$$\frac{dx}{dt} = (k_p + k_f)(1 - x)\lambda_0 \tag{1}$$

$$\frac{d[\mathrm{I}]}{dt} = -r_i - \frac{[\mathrm{I}]}{V}\frac{dV}{dt} \tag{2}$$

$$\frac{d[\mathrm{S}]}{dt} = -\frac{[\mathrm{S}]}{V}\frac{dV}{dt} \tag{3}$$

$$\frac{d\lambda_i}{dt} = r_{\lambda_i} - \frac{\lambda_i}{V}\frac{dV}{dt} \qquad \text{for } i = 0, 1, 2 \tag{4}$$

$$\frac{d\mu_i}{dt} = r_{\mu_i} - \frac{\mu_i}{V}\frac{dV}{dt} \qquad \text{for } i = 0, 1, 2 \tag{5}$$

$$\frac{dV}{dt} = -\frac{V_0}{(1 + \beta)}\left[\epsilon\frac{dx}{dt} + x\frac{d\epsilon}{dt}\right] \tag{6}$$

where

$$V = V_0(1 - \epsilon x + \beta)/(1 + \beta) \tag{7}$$

$$r_i = k_d[\mathrm{I}] \tag{8}$$

$$r_{\lambda_0} = 2fk_d[\mathrm{I}] - k_t\lambda_0^2 \tag{9}$$

$$r_{\lambda_1} = 2fk_d[\mathrm{I}] - k_t\lambda_0\lambda_1 + (k_s[\mathrm{S}] + k_p[\mathrm{M}])(\lambda_0 - \lambda_1) + k_f[\mathrm{M}]\lambda_0 \tag{10}$$

$$r_{\lambda_2} = 2fk_d[\mathrm{I}] - k_t\lambda_0\lambda_2 + k_s[\mathrm{S}](\lambda_0 - \lambda_2) + k_p[\mathrm{M}](2\lambda_1 + \lambda_0) + k_f[\mathrm{M}](\lambda_0 - \lambda_2) \tag{11}$$

$$r_{\mu_0} = \left(k_{td} + \frac{1}{2}k_{tc}\right)\lambda_0^2 + (k_f[\mathrm{M}] + k_s[\mathrm{S}])\lambda_0 \tag{12}$$

$$r_{\mu_1} = k_t\lambda_0\lambda_1 + (k_f[\mathrm{M}] + k_s[\mathrm{S}])\lambda_1 \tag{13}$$

$$r_{\mu_2} = k_t\lambda_0\lambda_2 + k_{tc}\lambda_1^2 + (k_f[\mathrm{M}] + k_s[\mathrm{S}])\lambda_2 \tag{14}$$

However, at high conversions, entanglements are likely to slow significantly the translational motion of growing radicals, suggesting the rate of termination may then be dominated by translational diffusion. Onset of the gel effect is likely linked to a switch in rate-limiting diffusion step. This is supported by the theoretical work of Tulig and Tirrell[17] and Mahabadi and O'Driscoll.[53]

Despite the existence of two diffusion-controlled regions, many investigators continue to ignore the segmental controlled regime. Quantitative results are obtained because the actual termination rate does not vary significantly from a constant one at low conversion. Hence only the translational diffusion-controlled regime need be modeled for the gel effect. Translational diffusion is directly related to the self-diffusivity of the macroradicals in the reacting solution. Three major theories are currently used to describe the self-diffusion coefficient of polymer molecules. These are (1) Bueche's diffusion theory,[54] (2) free volume theory,[55,56] and (3) reptation theory.[57]

Bueche's diffusion model requires an accurate viscosity model to be of use. Free volume theory suffers from its semiempirical nature, while reptation has only been extended to polydisperse stress–strain calculations. Only free volume theory is applicable over the whole range of conversion, but it alone cannot correctly predict the gel effect. This has led to model

TABLE V
Rate Constants and Physical Properties[13,17,22,43-51]

$f = 0.58$ for AIBN $\quad f = 1.0$ for BPO

$k_d = 6.32 \times 10^{16} \exp([-30.66 \text{ kcal/mol}]/RT_k)$ (min^{-1}) AIBN

$k_d = 1.014 \times 10^{16} \exp([-30.0 \text{ kcal/mol}]/RT_k)$ (min^{-1}) BPO (Tobolsky and Baysal, 1953[43])

$k_p^0 = 2.95 \times 10^7 \exp([-4.35 \text{ kcal/mol}]/RT_k)$ (L/mol min) (Mahabadi and O'Driscoll, 1977[44])

$\frac{k_f}{k_p} = 9.48 \times 10^3 \exp([-13.88 \text{ kcal/mol}]/RT_k)$ (Stickler and Meyerhoff, 1978[45])

$\frac{k_s}{k_p} = 1.01 \times 10^3 \exp([-11.40 \text{ kcal/mol}]/RT_k)$ (Gopalan and Santhappa, 1957[46])

$k_t^0 = 5.88 \times 10^9 \exp([-0.701 \text{ kcal/mol}]/RT_k)$ (L/mol min) (Mahabadi and O'Driscoll, 1977[44])

$\frac{k_{tc}}{k_{td}} = 3.956 \times 10^{-4} \exp([4.09 \text{ kcal/mol}]/RT_k)$ (Bevington et al., 1954[22])

$\rho_m = 0.968 - 1.225 \times 10^{-3} T_c$ (g/cm^3) (Tulig and Tirrell, 1981[17])

$\rho_p = 1.2$ (g/cm^3) (Brandup and Immergut, 1975[47])

$\rho_s = 0.883 - 9 \times 10^{-4} T_c$ (g/cm^3) (Baillagou, 1983[48])

$Cp_m = Cp_p = 0.4$ (cal/g °C) (Jaisinghani and Ray, 1977[49])

$Cp_s = 0.535$ (cal/g °C) (Perry and Chilton, 1974[50])

$mw_m = 100.13$ (g/mol) (Weast, 1982[51])

$mw_s = 92.14$ (g/mol) (Weast, 1982[51])

$v_m = 0.025 + 0.001(T_c + 106)$ (Balke and Hamielec, 1973[13])

$v_p = 0.025 + 0.00048(T_c - 114)$ (Balke and Hamielec, 1973[13])

$v_s = 0.025 + 0.001(T_c + T_{gs})$

$T_{gs} = 102$°C (benzene); 160°C (toluene); 92°C (ethyl acetate)

$$\Phi_m = \frac{(1 - x)}{(1 - \epsilon x + \beta}$$

$$\Phi_p = \frac{x(1 - \epsilon)}{(1 - \epsilon x + \beta)}$$

$$\Phi_s = \frac{\beta}{(1 - \epsilon x + \beta)}$$

$\rho = \rho_m \Phi_m + \rho_p \Phi_p + \rho_s \Phi_s$

$Cp = Cp_m \Phi_m + Cp_p \Phi_p + Cp_s \Phi_s$

$v_f = v_m \Phi_m + v_p \Phi_p + v_s \Phi_s$

where

ρ = density of reacting mixture
ρ_m = density of monomer
ρ_p = density of polymer
ρ_s = density of solvent
Cp = heat capacity of reacting mixture
Cp_m = heat capacity of monomer
Cp_p = heat capacity of polymer
Cp_s = heat capacity of solvent
v_f = free volume of reacting mixture
v_m = free volume of monomer
v_p = free volume of polymer
v_s = free volume of solvent
Φ_m = volume fraction of monomer
Φ_p = volume fraction of polymer
Φ_s = volume fraction of solvent
T_k = temperature (°K)
T_c = temperature (°C)

segmentation, where arbitary switch points are used to "turn on" diffusive limitation. Lumped constants are frequently used due to a lack of reliable diffusion data. Model parameters are adjusted to match existing experimental data.

Most gel effect models were originally developed for the bulk polymerization of methyl methacrylate. Only four, Cardenas and O'Driscoll,[4] Martin and Hamielec,[12] Schmidt and Ray,[58] and Soh and Sundberg,[59] have been specifically tested for solution polymerization. However, these models are not without limitations. COD and SS are not diffusion-based models, and SR and MH have critical break points which are not desirable for our subsequent process optimization calculations. Hence, it was decided to modify and improve an existing model—the CCS model for solution polymerization.

Derivation of the CCS model is described in the paper by Chiu et al.[42] and is summarized below. The region around a given radical can be divided into three zones (see Fig. 2). Beyond a distance r_b, the concentration of radicals, C_b, is that of the bulk phase. To terminate, another radical must diffuse or propagate from the bulk to within a minimum separation distance r_m for both radicals to collide. An effective diffusion coefficient D_{eff} is used to embody both translational and segmental diffusion prior to eventual biradical collision.

The rate of radical transport into the reaction zone ($r \leqslant r_m$) must equal the rate of radical consumption, R_t. This can be mathematically stated as

$$4\pi r_m^2 D_{\text{eff}} \frac{dC}{dr} = R_t \tag{11}$$

Assuming $r_b >> r_m$ and R_t is independent of r, eq. (11) can be integrated between r_b and r_m to yield

$$4\pi D_{\text{eff}} r_m (C_b - C_m) = \frac{4}{3}\pi r_m^3 k_t^0 C_m C_b \tag{12}$$

where k_t^0 is the true termination rate constant and C_m is the effective concentration of radicals in the reaction zone. Equation (12) can be rear-

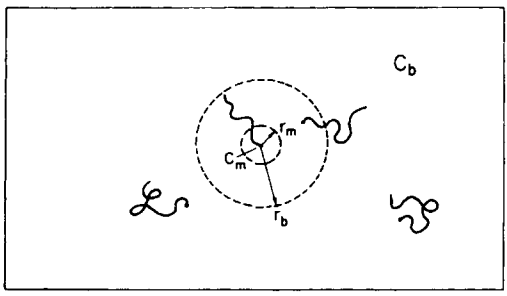

Fig. 2. Reaction coordinate system for free-radical termination. C_b is the bulk radical concentration, and C_m is the hypothetical radical concentration surrounding the immediate vicinity of the central radical.

ranged to solve for C_m:

$$C_m = \frac{D_{\text{eff}} C_b}{D_{\text{eff}} + \frac{1}{3} r_m^2 k_p^0 C_b} \tag{13}$$

Since termination only occurs in the reaction zone, the overall termination rate is the same as the local termination rate:

$$k_t C_b^2 = k_t^0 C_m C_b \tag{14}$$

where k_t is the apparent termination rate constant. Inserting eq. (13) into eq. (14) and rearranging terms yield

$$\frac{1}{k_t} = \frac{1}{k_t^0} + \frac{r_m^2 C_b}{3 D_{\text{eff}}} = \frac{1}{k_t^0} + \frac{r_m^2 C_b}{3 D_0 C} = \frac{1}{k_t^0} + \Theta_t \frac{\lambda_0}{C} \tag{15}$$

where D_{eff} is evaluated by the Fujita–Doolittle equation and separated into a concentration dependent term C and a molecular weight term D_0.[55,56] Notice that Θ_t has units of time, and is a measure of the relative importance of diffusive resistance vs. reactive resistance in contributing to the overall resistance toward biradical termination.

A similar analysis can be done for the propagation reaction. This leads to

$$\frac{1}{k_p} = \frac{1}{k_p^0} + \frac{r_m^2 C_b}{3 D_{\text{eff}}} = \frac{1}{k_p^0} + \frac{r_m^2 C_b}{3 D_0 C} = \frac{1}{k_p^0} + \Theta_p \frac{\lambda_0}{C} \tag{16}$$

These final results show that the overall rate of chain propagation and termination can be viewed as the sum of a reaction-limited term and a diffusion-limited term. The concept of r_m can be related to the Smoluchowski capture radius. The Smoluchowski equation is[21]

$$\frac{1}{k_t} = \frac{1}{k_t^0} + \frac{1}{8\pi r_c D_{\text{translation}}} \tag{17}$$

where r_c is the Smoluchowski capture radius. Comparing eq. (17) with eq. (16),

$$r_c = \frac{3 D_{\text{eff}}}{8\pi r_m^2 \lambda_0 D_{\text{translation}}} \tag{18}$$

Since accurate data on the capture radius is scare, Θ_t and Θ_p are treated as adjustable parameters in the model.

Θ_t should be a function of temperature and the average molecular weight of the polymer formed as well as the chain length of the diffusing radicals. However, because of the complicated nature of the termination process, Θ_t does not assume any obvious form. Instead, for batch processes, it was proposed to correlate Θ_t with the initial initiator loading I_0. This works well

as the kinetic chain length is inversely proportional to the square root of the initiator concentration. A simple power dependence of the form

$$\Theta_t = \frac{A}{I_0^a} \exp\left(\frac{\Delta E}{RT}\right) \tag{19}$$

is proposed. The activation energy ΔE was found previously.[42]

To determine the power a, model predictions are fitted to a large collection of conversion-time data.[13,25,41] A plot of log (Θ_t) vs. log (I_0) yields the power a as the slope of the correlation (see Fig. 3).

The slope suggests that a first power dependence on I_0 exists over the most likely range of initiator concentrations. Figure 4 shows the comparison of the model with the experimental data of Ito.[25] The data are not fitted as well for high I_0, suggesting a different dependence at very low molecular weights. The first power dependence is not entirely applicable for strong nonisothermal behavior since appreciable changes in initiator concentration may occur. Fortunately, in these cases, thermal effects dominate over the gel effect. Θ_p was found to vary strongly only with temperature and an Arrhenius-type rate expression is used to correlate this parameter.

Extension of the CCS model to solution polymerization is straightforward. Only a single modification is needed. Φ_m in the Fujita–Doolittle equation

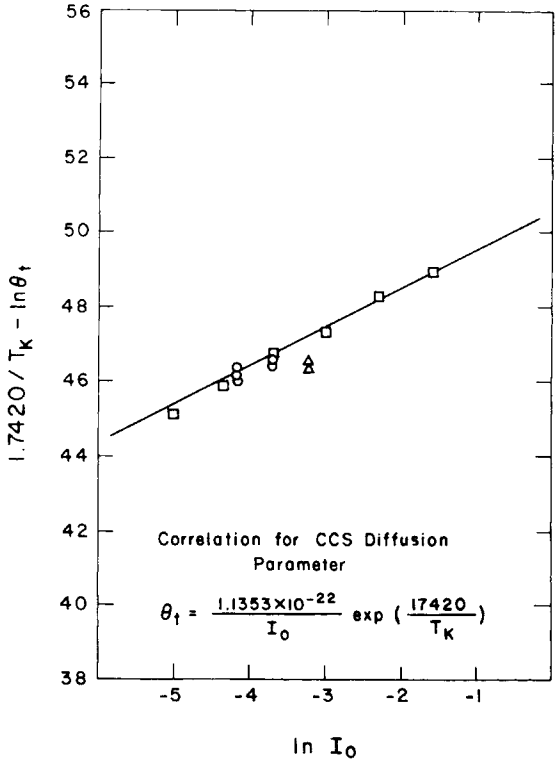

Fig. 3. Results of curve fitting literature data to determine Θ_t as a function of initiator loading. (□) Ito[25]; (○) Balke and Hamielec[13]; (△) Schultz and Harborth.[41]

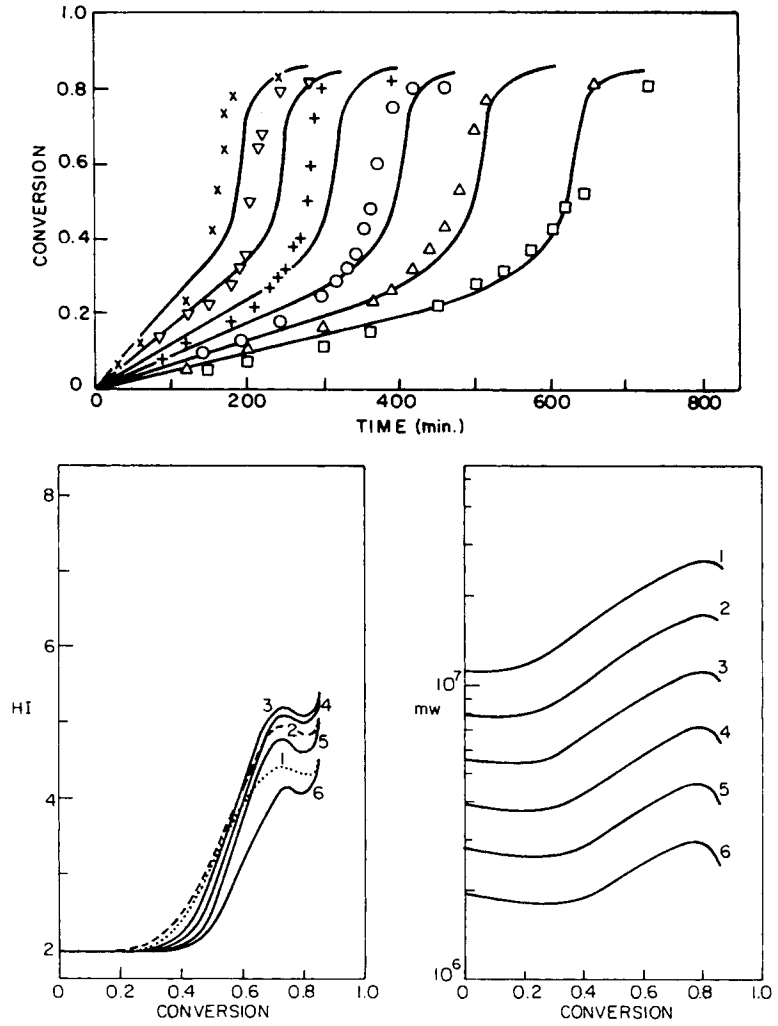

Fig. 4. Model comparison with the bulk polymerization data of Ito (1975)[25] at 45°C. Good agreement is obtained over a wide range of AIBN loadings. Onset of the gel effect shifts to low conversions as the initiator loading decreases. Also shown are the predicted molecular weights and heterogeneity indices as functions of conversion at different initiator loadings. Top: I_0 (*M* AIBN): (X) 0.2; (▽) 0.1; (+) 0.05; (○) 0.025; (△) 0.0125; (□) 0.00625.Bottom: (*M* AIBN): (1) 0.00625; (2) 0.0125; (3) 0.025; (4) 0.05; (5) 0.1; (6) 0.2.

can be replaced by $(1 - \Phi_p)$ if both monomer and solvent are treated as diluents. Specific solvent characteristics, such as solvation strength for the particular polymer under consideration, are ignored in this model. The complete CCS model is summarized in Table VI. Model predictions are discussed in a later section.

MODELING THE MWD

The molecular weight distribution of the polymer chains formed during polymerization is directly related to the entire history of reaction kinetics through the polymer mass balance equations in Table IV.

TABLE VI
Constitutive Gel and Glass Effect Equations

$$\frac{k_t}{k_t^0} = \frac{C}{C + \theta_t k_t[\lambda_0]}$$

$$\frac{k_p}{k_p^0} = \frac{C}{C + \theta_p k_p[\lambda_0]}$$

where

$$C = \exp\left[\frac{(1 - \Phi_p)}{A + B(1 - \Phi_p)}\right]$$

$$A = 0.168 - 8.21 \times 10^{-6}(T_c - 114)^2$$

$$B = .03$$

$$\theta_p = 5.4814 \times 10^{-16} \exp(13982/T_k)$$

$$\theta_t = \frac{1.1353 \times 10^{-22}}{[I_0]} \exp(17420/T_k)$$

$[I_0]$ = initiator loading [mol/L]

Three distinct distributions are possible from these equations. They are the (1) instantaneous (or live radical), (2) dead polymer, and (3) cumulative MWDs. It is the cumulative distribution which determines most of the properties, and is the one that must be controlled. Unless otherwise stated, we will simply refer to the cumulative MWD as the MWD.

In order to determine these distributions, it is important to know the average radical (or kinetic chain) length ν. This length is a measure of the instantaneous molecular weight being produced at any instant. It can be found from

$$\frac{1}{\nu} = \frac{(fk_dk_t[I])^{1/2}}{k_p[M]} + B_s\frac{[S]}{[M]} + B_m \tag{20}$$

where $B_s = k_s/k_p$ and $B_m = k_f/k_p$. In deriving eq. (20), the QSSA is made for all radicals.

One obvious method of modeling the MWD is to directly integrate the polymer mass balance equations for a large, but finite, number of chain lengths. The polymer concentrations then yield the MWD. Liu and Amundson[60] solved over 200 nonlinear first-order ODEs assuming a limiting chain length of 100. But chain lengths of the order of 10^4 are not uncommon for PMMA. Another approach is to convert the infinite number of mass balance equations into a single ODE by the use of a generating function or Z-transform. Ray[61] has demonstrated the utility of this method for the batch polymerization of styrene. When the average chain length is long, the discrete distribution of polymer concentrations can also be approximated by a continuous one. This collapses the various radical species balances into a single PDE with respect to the chain length. The dead polymer balances may similarly be collapsed into another first order PDE and solved. Zeman and Amundson[62] and Mimasu and Ayabe[63] did parametric studies of the effect of temperature, initiator loading, and monomer concentration on the MWD with this technique. Coyle et al.[64] investigated the effect of chain length dependence on diffusion and the onset of entanglement using a finite element technique to solve their nonlinear PDEs.

The MWD can also be solved by statistical methods. Work in this area was pioneered by Kuhn,[65] Schultz,[66] and Flory,[67] who viewed chain propagation as a stochastic process with different possible probabilities arising from kinetic mechanism. The probability of propagation is given by

$$\alpha = \frac{k_p[\mathrm{M}]}{k_p[\mathrm{M}] + k_s[\mathrm{S}] + k_f[\mathrm{M}] + k_t[\lambda_0]} \tag{21}$$

Then, the probability (or mole fraction) of having a radical of chain length n is simply

$$\frac{n_i}{N} = (1 - \alpha)\alpha^{(i-1)} \tag{22}$$

where n_i is number of radicals of length i and N is the total number of radicals. The instantaneous MWD can then be easily found by varying i. Equation (22) is also called the "most probable" or "geometric" distribution. Kinetic rate constants for eq. (21) can be found in Table V. Model equations for the concentrations and the gel effect can be found in Tables IV and VI.

In free radical, chain addition polymerization, α is close to 1, so that long chains are formed even at low conversions. Equation (22) can be further simplified by noting that $1/\alpha = 1 + 1/\nu$ and $ln\ \alpha \simeq (1 - \alpha)$. This leads to the expression

$$\frac{n_i}{N} = \frac{1}{\nu} \exp\left(\frac{-\mathrm{i}}{\nu}\right) \tag{23}$$

which makes it apparent that monomers (radicals of chain length 1) will always be the most numerous molecules in the instantaneous MWD.

However, monomers only occupy a fraction of the weight of the distribution. Another common way of looking at the same distribution is to weigh each concentration by its molecular weight. This can be done by noting that

$$\frac{w_i}{W} = \frac{N}{N_0}\frac{n_i}{N}\frac{i\ \mathrm{mw}_m}{\mathrm{mw}_m} = \frac{\text{wt of } i\text{-mer}}{\text{wt of all radicals}} \tag{24}$$

where mw_m is the molecular weight of monomer and N_0 is the initial number of chains. But since monomers are considered as radicals of length 1,

$$\alpha = \frac{\text{no. of chain propagating}}{\text{initial no. of chains}} = \frac{N_0 - N}{N_0} \tag{25}$$

Inserting Equations (22) and (25) into (24) and simplifying yields the most probable weight fraction distribution:

$$\frac{w_i}{W} = i(1 - \alpha)^2\, \alpha^{(i-1)} = \frac{i}{\nu^2} \exp\left(\frac{-i}{\nu}\right) \tag{26}$$

In this representation, the instantaneous MWD has a peak approximately about ν.

The number (NACL) and weight (WACL) average chain lengths can now be determined along with the statistical polydispersity. Since termination by disproportionation dominates, the instantaneous NACL is simply equal to the kinetic chain length, or $\bar{X}_n = \nu$. The instantaneous WACL, $\bar{X}_w$, is found from the number fraction distribution by

$$\bar{x}_w = \frac{\int_0^\infty (n_i/N) i^2 \, di}{\int_0^\infty (n_i/N) i \, di} = \frac{1 + \alpha}{1 - \alpha} \tag{27}$$

The instantaneous heterogeneity index (HI) or polymer polydispersity (PD) is then determined from

$$\text{HI (or PD)} = \bar{x}_w/\bar{x}_n = (1 + \alpha)/\alpha \tag{28}$$

Since α is always close to 1, the instantaneous MWD always has a statistical polydispersity near 2.

The cumulative MWD can then be determined by integrating the instantaneous MWD over all conversions and normalizing. If the weight fraction distribution is used,

$$\frac{W_i}{W} = \frac{1}{x} \int_0^x \frac{w_i}{W} dx \tag{29}$$

where W_i/W is the cumulative weight fraction distribution. This distribution can be directly used to compare with experimental GPC traces. The cumulative number ($\bar{X}_n$) and weight ($\bar{X}_w$) average chain lengths can both be found from the kinetic chain length by the following expressions[68]:

$$\bar{X}_n = \frac{x}{\int_0^x dx/\bar{x}_n} \tag{30}$$

$$\bar{X}_w = \frac{1}{x} \int_0^x 2\bar{x}_n \, dx \tag{31}$$

However, since w_i/W is a complex function of x, eq. (29) must be evaluated numerically. As an approximation, we can alternatively add subsequent instantaneous MWDs together to obtain the composite cumulative MWD. This approximation improves with decreasing step size in x. Likewise, the integrals in eqs. (30) and (31) can be replaced by a discrete summation to evaluate the cumulative NACL and WACL.

Figure 5 shows model predictions for several instantaneous and cumulative MWDs. Although the instantaneous MWD always has a polydispersity of 2, the cumulative distribution may be much larger than 2. Very

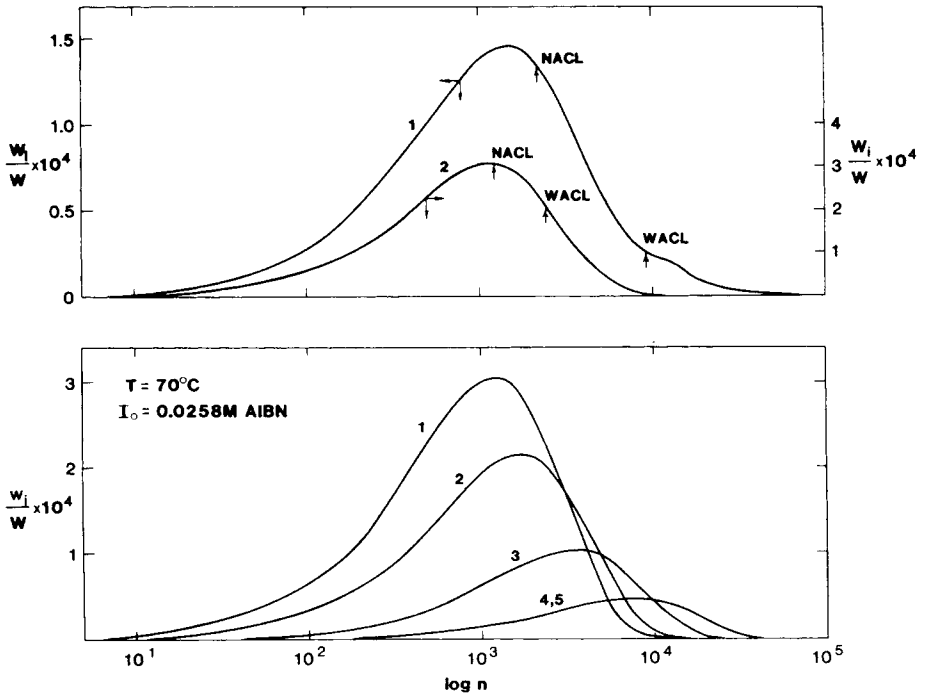

Fig. 5. Evolution of the instantaneous (w_i / W) and cumulative MWD (W_i / W) during the isothermal bulk polymerization of MMA. (T = 70°C, I_0 = 0.0258M AIBN) Notice the strong upward shift of the instantaneous MWD caused by the gel effect and how this shift broadens the cumulative MWD. Top: (x, $\overline{X}_n$, $\overline{X}_w$, HI): (1) 0.85, 2226, 9278, 4.17; (2) 0.10, 1232, 2466, 2.00. Bottom (x): (1) 0.1; (2) 0.3; (3) 0.4; (4) 0.5; (5) 0.7.

little broadening occurs at low conversions. However, a sharp shift in the instantaneous MWD toward higher molecular weights appears during the gel effect. This skews the MWD and causes a rapid increase in polymer polydispersity. Broadening of the MWD can be directly linked to changes in α. Even a small variation can have a profound affect on the kinetic chain length (and hence the instantaneous MWD) as can be seen in Table VII.

Addition of a solvent lowers the kinetic chain length by chain transfer, but eliminates the upward shift due to the gel effect. This narrows the MWD from 4.6 to almost 2. Once the gel effect is removed, broadening of the MWD occurs by concentration drift (f_s = 0.6 and 0.8). This drift results in a downward shift of the instantaneous MWD, with the NACL falling faster than the WACL as the polymerization proceeds. It is caused by the gradual decrease in the rate of propagation relative to the rate of termination and chain transfer. Thermal effects (or thermal drift) can shift the instantaneous MWD in either direction depending on the temperature change. Chain transfer to monomer does not appear to significantly affect the kinetic chain length during bulk polymerization.

Since the exact shape of the MWD is often not needed, the method of moments can be used to simplify calculations. These moments were defined in eqs. (3) and (4). However, the number of moments needed to uniquely describe the MWD depends on the accuracy desired. Bamford and Tompa[69]

TABLE VII
Influence of Concentration Drift on the Propagation Probability and the Kinetic Chain Length[a]

	Solvent fraction f_s				
X	0.0	0.2	0.4	0.6	0.8
0.1	0.99916 1202	0.99894 940	0.99855 692	0.99779 453	0.99554 223
0.3	0.99941 1697	0.99898 982	0.99838 616	0.99733 373	0.99438 177
0.5	0.99988 8007	0.99956 2266	0.99856 708	0.99672 304	0.99235 130
0.7	0.99988 8255	0.99982 5516	0.99917 1199	0.99599 248	0.98783 81
0.9	Glass	0.99940 1670	0.99909 1093	0.99330 148	0.96651 29
0.995	Glass	0.97485 39	0.98621 72	0.91292 11	0.60076 2
Cum. HI	4.6	3.0	2.2	3.2	4.0

[a] The upper value is the probability of propagation; the lower value is the kinetic chain length. $T = 70°C$ and $I_0 = 0.0258M$ AIBN.

found less than 1% error when 3 014 5 moments are used in conjunction with Laquerre polymomials to represent the MWD. Since only a rough estimate is needed, the polydispersity is quite adequate. Three live moments are enough to model the instantaneous MWD (see Fig. 6), while three dead moments are capable of handling the dead polymer MWD. The cumulative number ($\overline{M}_n$) and weight ($\overline{M}_w$) average molecular weights can then be found by

$$\overline{M}_n = (\lambda_1 + \mu_1)/(\lambda_0 + \mu_0) \tag{32}$$

$$\overline{M}_w = (\lambda_2 + \mu_2)/(\lambda_1 + \mu_1) \tag{33}$$

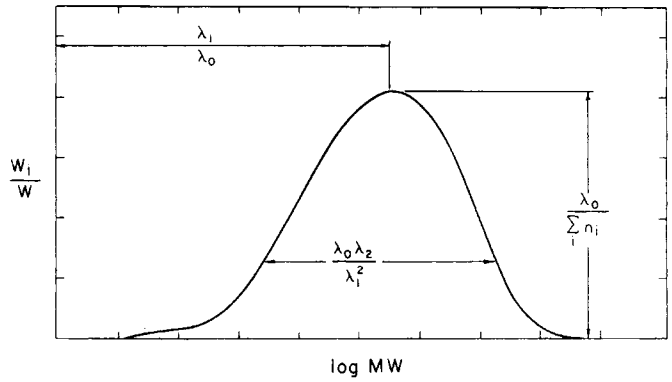

Fig. 6. The instantaneous MWD can be described by three moments. These are λ_0, λ_1, and λ_2. λ_0 is the total concentration of radicals. λ_1 along with λ_0 determines the average of the distribution. λ_2, λ_1, and λ_0 used together give a measure of the breadth the distribution. The cumulative MWD can be described in a similar way.

with the cumulative polymer polydispersity given by

$$\mathrm{HI} = \frac{(\lambda_2 + \mu_2)(\lambda_0 + \mu_0)}{(\lambda_1 + \mu_1)^2} \tag{34}$$

The variance δ of the MWD is then related to the polydispersity and the number average molecular weight by

$$\mathrm{HI} = 1 + (\delta/\overline{M}_n)^2 \tag{35}$$

Hence, most of the information about the evolution of the MWD can be obtained without having to generate the entire distribution itself. This will considerably simplify mathematical calculations to determine optimal control strategies for the MW and MWD.

ISOTHERMAL MODEL PREDICTIONS

Comparison of the model under isothermal bulk conditions with the experimental data of Balke and Hamielec[13] and Ito[25] is shown in Figures 4 and 7. A comparison with the solution data of Schultz and Harborth[41] is shown in Figures 8 and 9. Bulk polymer conversion increases fairly linearly with time until the onset of the gel effect. Autoacceleration of the reaction rate then carries the reaction to the limiting conversion. Addition of a solvent delays and moderates the gel effect. The fit to the experimental data is not as good at high solvent fractions or high initiator loadings. Under these conditions, short chains are produced and radical mobility is underpredicted by the model.

Molecular weight predictions are shown in Figures 4, 7, and 8. Polymer molecular weight drops slightly due to volume contraction at low conversion. This contraction raises the effective initiator concentration and lowers the instantaneous (and hence the cumulative) MW. Onset of the gel effect marks the production of longer polymer chains and an upswing in both $\overline{M}_n$ and $\overline{M}_w$. Molecular weights level off and fall as limiting or complete conversion is approached due to concentration drift. This effect is not apparent in the bulk experimental data because glass formation freezes the polymerization reaction before significant amounts of low molecular weight material are produced. Onset of the gel effect shifts towards high conversions with increasing initiator concentration. Addition of a solvent decreases the gel effect and reduces the amount of high molecular weight material produced.

The effect of varying the ratio of disproportionation to combination is seen in Figure 7. Since k_{td}/k_{tc} varies with temperature, higher ultimate polydispersities are obtained with lower temperatures because combination raises $\overline{M}_w$ faster than disproportionation under the same conditions. Lower product molecular weights and shorter batch times are obtained at high temperatures. Thus, a tradeoff exists between minimizing the PD and reaching a desired MW. These observations are supported by the data of Balke and Hamielec,[13] but the scatter of the data points above the simulation

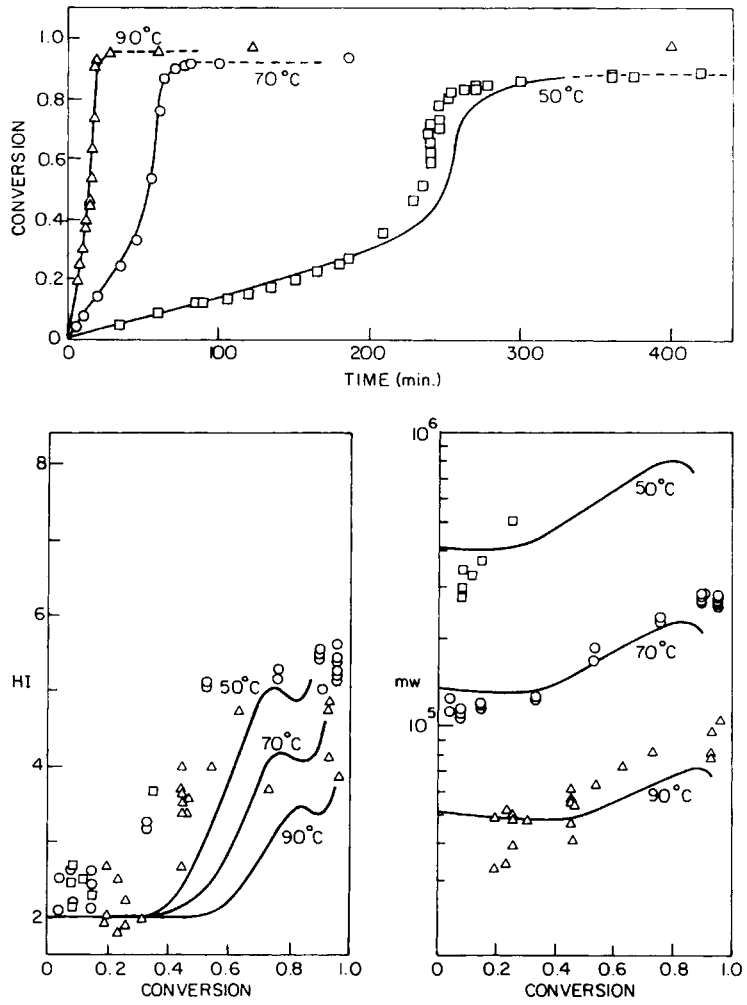

Fig. 7. Model comparison with the bulk polymerization data of Balke and Hamielec (1973)[13] at $I_0 = 0.0258M$ AIBN. Dashed lines indicate glass formation. Number average MW predictions are good, but changes in HI with temperature are over predicted (°C): (□) 50; (○) 70; (△) 90.

indicates a much weaker effect than predicted by the model (using the correlation obtained from the experimental data of Bevington et al.[22]).

Model simulations also predict a slight variation in the ultimate polymer PD with varying initiator concentration as shown in Figure 4. Lower polydispersities are obtained at either very high or very low initiator loadings. As I_0 increases, the interval between k_p and k_t declines is shortened (onset of the gel effect is shifted closer to the onset of the glass effect). This produces fewer longer chains and lowers PD. As I_0 decreases, high MW polymer can be produced from the start. The gel effect still produces longer chains, but $\overline{M}_w$ is now harder to shift upward at low I_0. This lowers PD again. While this effect exists, it is obscured by the scatter in the data of Balke and Hamielec.[13] Nevertheless, it appears that most of the important features of MMA polymerization have been correctly incorporated into the model.

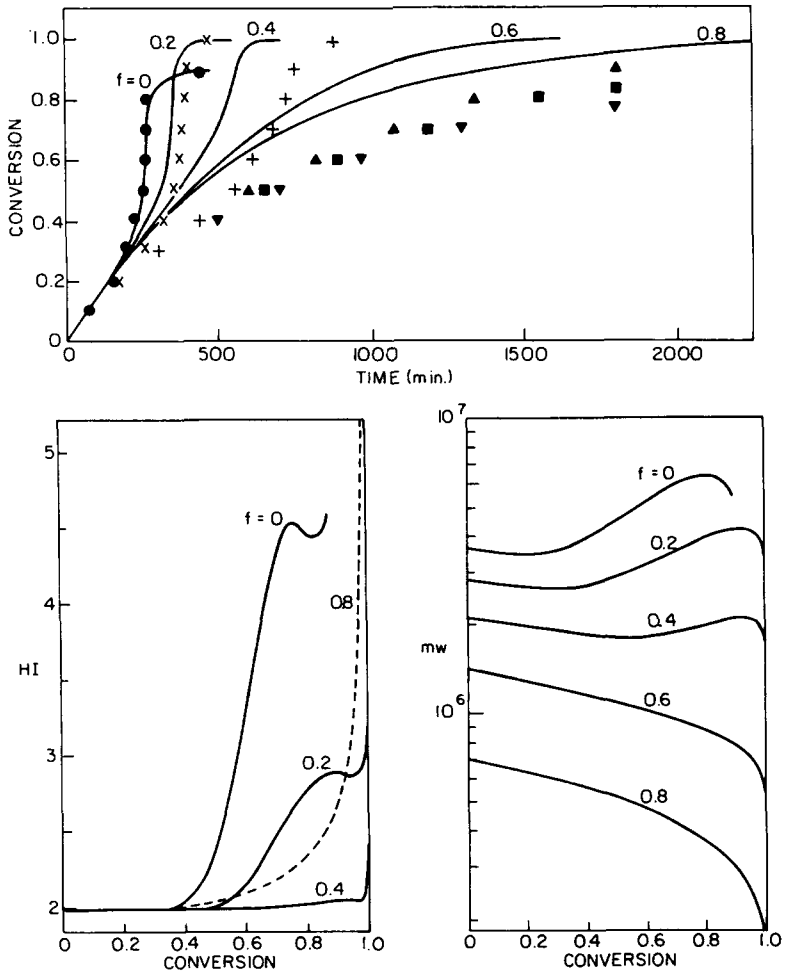

Fig. 8. Model comparison with the solution polymerization data of Schultz and Harborth (1947).[41] Benzene is the solvent. MMA is polymerized at 50°C with 0.0413*M* BPO. Polymerization rates decrease with increasing dilution of the monomer. Actual amounts of polymer formed have been normalized by defining the conversion as the weight of polymer over the initial weight of monomer. Also shown are the predicted molecular weights and heterogeneity indices as functions of conversion at different batch solvent fractions. Top (f_s): (●) 0; (x) 0.2; (+) 0.4; (▲) 0.6; (■) 0.8; (▼) 0.9.

NONISOTHERMAL BEHAVIOR

One of the most difficult aspects of polymerization is that it is exothermic. Large quantities of heat are released which must be either removed by a coolant or dissipated to the surroundings. Since heat removal from a viscous mixture is difficult, high temperatures are often encountered. Under the right conditions, polymerizing reactors can thermally run away when the temperature feeds back to increase reaction rates which further raise the temperature. Even if runaway does not occur, high temperatures can cause thermal drift which broadens the molecular weight distribution. This can crucially affect end product properties.[70]

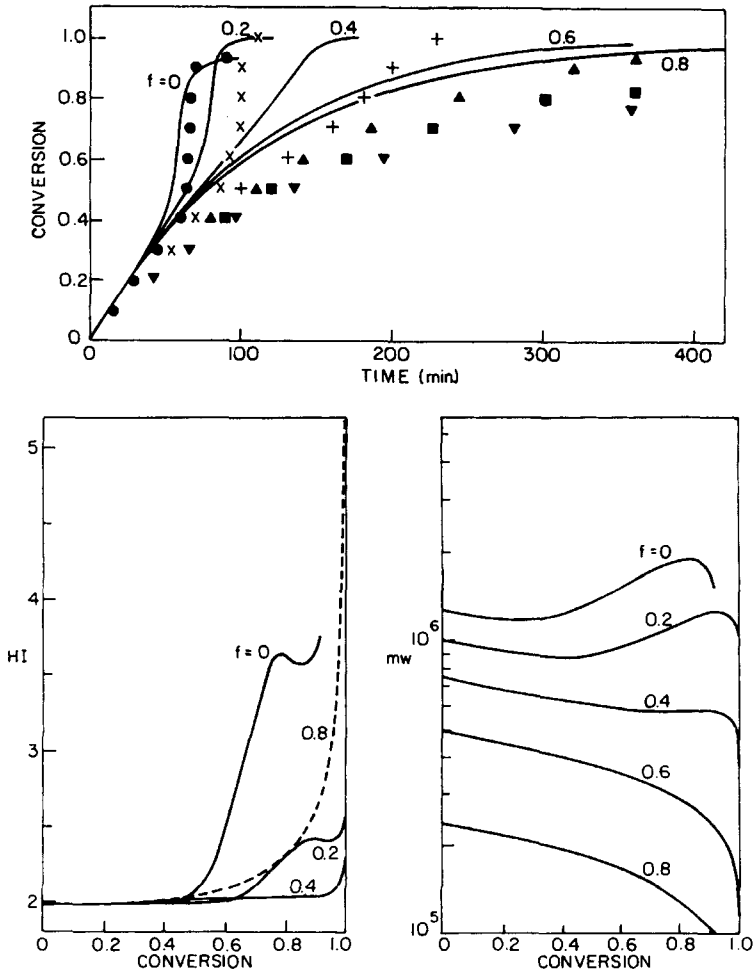

Fig. 9. Model comparison with the solution polymerization data of Schultz and Harborth (1947).[41] MMA is again polymerized in benzene at 70°C with 0.0413*M* BPO. Increasing solvent fraction reduces the gel effect and decreases HI. Chain transfer to solvent also reduces MW. Top (f_s): (●) 0; (x) 0.2; (+) 0.4; (▲) 0.6; (■) 0.8; (▼) 0.9.

Nonisothermal polymerization can be modeled with the addition of an energy balance equation. Such an expression is shown below for an ideally mixed batch reactor

$$\rho \mathrm{Cp}\, V\frac{dT}{dt} = (-\Delta H_p)k_p[\mathrm{M}][\lambda_0] - UA(T - T_s) \tag{36}$$

where U is the overall heat transfer coefficient, A is the available heat transfer area, and V is the reaction mass and Cp is the heat capacity of the reacting mixture. Heat generation and heat removal are represented by the first and second terms on the right-hand side of eq. (36). For simplicity, the reactor wall will be assumed to be maintained at temperature T_s, the surrounding temperature.

The reactor temperature falls when $dT/dt < 0$ and rises when $dT/dt > 0$. A steady state temperature is obtained when $dT/dt = 0$. If the reactor temperature rises, it does not increase without bound. If the system is under atmospheric pressure or partially pressurized, reaction temperatures will increase until the boiling point of the monomer (as determined by the Antoine equation) is reached,[48] and then level off. The latent heat of vaporization of the monomer is then used to remove the heat of reaction. Reflux condensers are often employed to condense the evaporated monomer and return it to the reactor.[71] This process is modeled by setting $dT/dt = 0$ once the monomer boiling point is reached. The normal boiling point of MMA is 100°C.

If the system is completely pressurized, then either the adiabatic temperature rise T_a or the ceiling temperature T_c will limit the polymerization process. The adiabatic temperature rise is determined from

$$T_a = T_0 + m(-\Delta H_p)/M\,\mathrm{Cp} \tag{37}$$

where ΔH_p is the heat of polymerization, m is the initial amount of monomer, M and Cp are the mass and heat capacity of the reacting mass, and T_0 is the initial temperature. A rise of 260°C is possible for MMA under bulk conditions.

At very high temperatures, PMMA begins to decompose into shorter oligomeric fragments. Dainton and Ivin[72] has defined T_c as the temperature at which the rate of depolymerization equals the rate of chain propagation. Above T_c, it is no longer possible to produce PMMA. Under conditions of propagation–depolymerization, the ceiling temperature may be expressed as

$$T_c = \frac{\Delta H_p}{(\Delta S_p^0 + R_g \ln[\mathrm{M}])} \tag{38}$$

where ΔS_p^0 is the entropy of the reaction, R_g is the ideal gas constant, and [M] is the concentration of monomer. Values for ΔH_p and ΔS_p^0 were found in Dainton and Ivin[72]. Figure 10 shows a plot of the ceiling temperature as a function of conversion. Absolutely complete conversion does not appear theoretically possible, even in the absence of the glass effect, because of the logarithmic dependence on [M].

Equation (38) is derived by assuming Arrhenius-type rate constants for k_p and k_{de} and noting that $\Delta H_p = E_{de} - E_p$ and $\Delta S_p^0 = R_g \ln (A_p/A_{de})$. Working backwards from literature values for ΔS_p^0 and δH_p, the depolymerization rate constant is found to be

$$k_{de} = 3.888 \times 10^{13} \exp(-18253/RT_k)\ (1/\mathrm{min}) \tag{39}$$

as $k_p \simeq k_p^0$ at high temperatures. Incorporating depolymerization into eq. (21) and normalizing with respect to the rate of propagation yields the

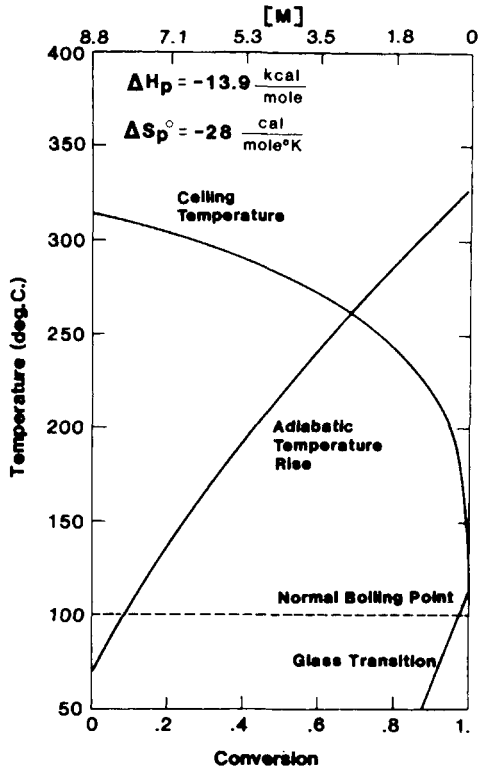

Fig. 10. Upper limits on the temperature and conversion obtainable during the bulk polymerization of MMA. Formation of a glass stops all reaction when $T < 114$°C. The adiabatic temperature rise curve starts at 70°C, the initial temperature for most of the experimental and theoretical work done in this study. A pressurized reactor is required to operate above the normal boiling point of MMA.

following expression:

$$\alpha = \frac{B_p}{B_p + B_f + B_t + B_{de}} \tag{40}$$

where $B_p = 1$, $B_f = k_f/k_p$, $B_t = k_t\,[\lambda_0]/k_p[\mathrm{M}]$, and $B_{de} = k_{de}/k_p[\mathrm{M}]$. This equation can then be used to determine the importance of depolymerization on the rate of polymerization. Using the rate expressions in Table VI and the CCS gel effect model, the following list of ratios was obtained for bulk polymerization at $x = 0.1$ and $I_0 = 0.0258$M AIBN.

T(°C)	ν	B_p	B_t	B_f	B_{de}
120	88	1	7.0×10^{-3}	3.5×10^{-4}	3.3×10^{-3}
140	40	1	0.016	7.9×10^{-4}	8.1×10^{-3}
160	20	1	0.031	1.7×10^{-3}	0.018
180	10	1	0.058	3.3×10^{-3}	0.039
200	5	1	0.102	6.3×10^{-3}	0.077

From these results, depolymerization does not become significant compared to termination and propagation until very high temperatures are reached. Hence, depolymerization may be ignored as long as the ceiling temperature is not closely approached.

Thermal drift of the instantaneous MWD occurs because the rate constants vary differently with temperature. This directly affects α and ν and broadens the MWD. Biesenberger and Capinpin[73] have extensively studied drift behavior and classified their results in three categories: (1) conventional, (2) gel effect or weak dead-ending, and (3) dead-ended. Conventional polymerizations are those where concentration drift dominates the instantaneous MWD. Dead-ending occurs whenever the rate of initiator consumption is greater than or comparable to the rate of propagation. Dead-ending may be induced by high temperatures since initiator decomposition increases exponentially with temperature. Polymerization then stops when all the initiator is "burned out."[74]

In conventional polymerization, ν always drifts downward and shifts the instantaneous MWD toward lower MWs. In dead-ended polymerizations, ν drifts upward under isothermal conditions. Longer chains are formed as the initiator concentration drops. However, under nonisothermal conditions, dead-ending leads to a downward shift in ν. The higher temperatures allow for a larger steady-state radical population due to accelerated initiator decomposition, and this results in the formation of shorter chains. In conventional polymerizations with gel effect, ν first drops until the onset of the gel effect, and then shifts upward as hindered termination occurs. Regardless of the direction of the drift, the polydispersity always increases.

Thermal runaway occurs whenever $dT/dt >> 0$ and d^2T/dt^2 does not show an inflection before dead-ending or limiting conversion is reached.[75] Under these conditions, progressively higher temperatures are reached until one of the aforementioned limits is reached. A special kind of runaway is thermal ignition. Thermal ignition show parametric sensitivity and may occur in batch and semibatch reactors and in the steady state behavior of continuous reactors. It is very difficult to control as small perturbations in either temperature or reactant concentrations will result in thermal runaway.

Biesenberger et al.[76] studied the effects of thermal runaway on the polymer polydispersity for batch reactors. They found that conventional polymerizations produced narrower polymers under near-isothermal conditions than under runaway conditions. Borderline dead-ended (or gel effect) polymerizations tended to follow the same trend, but produced narrower polymers than the corresponding conventional case. Surprisingly, strong dead-ended polymerizations were found to produce narrower polymers under runaway conditions than under near-isothermal conditions.

Figures 11 and 12 show the effect of the overall heat transfer coefficient for a pressurized 1-L spherical reactor. As expected, thermal runaway led to dead-ending and premature limiting conversions. Molecular weights drift downward with increasing reactor temperature with adiabatic conditions producing the lowest MW and the largest PD. As heat transfer improves, complete (or limiting for bulk polymerization) conversion is reached. Mo-

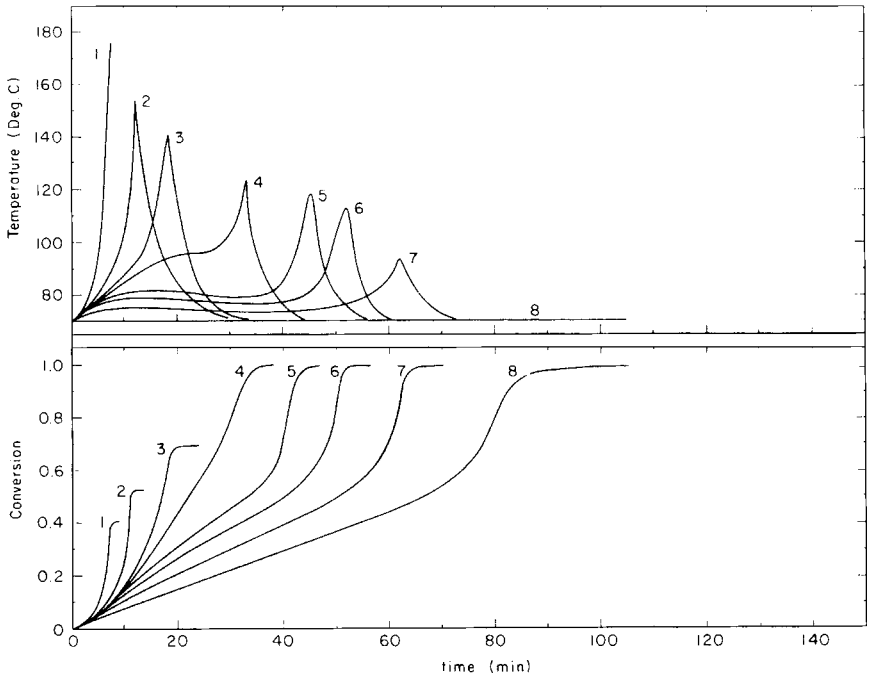

Fig. 11. Nonisothermal solution polymerization of MMA in 20% toluene. Influence of heat transfer on the conversion and temperature. T_s = 70°C, V_0 = 0.5 L, I_0 = 0.0258M AIBN, and A = 483.6 cm²; multiply U (Btu/h ft² °F) by 4.88 to convert to U (kcal/h m² °C): (1) 0; (2) 10; (3) 13.75; (4) 15; (5) 17.5; (6) 20; (7) 30; (8) ∞.

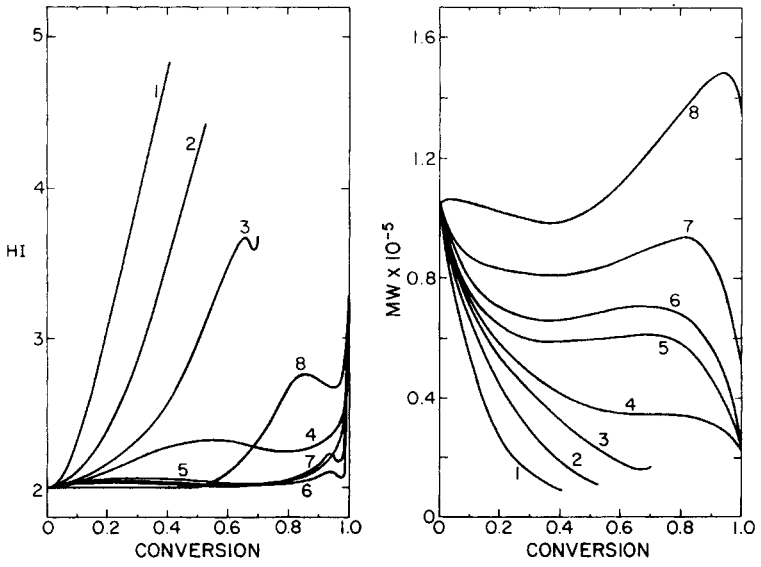

Fig. 12. Nonisothermal solution polymerization of MMA in 20% toluene at 70°C and I_0 = 0.0258M AIBN. HI decreases as the thermal effects dominate over the gel effect, but increases again as adiabatic conditions are reached. MW decreases with decreasing heat transfer. U(Btu/h ft² °F): (1) 0; (2) 10; (3) 13.75; (4) 15; (5) 17.5; (6) 20; (7) 30; (8) ∞.

lecular weights then drift upward at higher conversions when the gel effect dominates at near-isothermal conditions. Batch processing times are shortened by the higher temperatures, but at the expense of producing lower molecular weights.

CONCLUSION

In summary, contemporary gel effect models and their theoretical foundations have been reviewed. A detailed mathematical model previously developed for bulk polymerization of MMA has been extended to describe solution polymerizations. This model has been carefully validated for a range of experimental conditions and found to provide adequate conversion and molecular weight predictions. This kinetic model will provide the basis for a theoretical and experimental investigation of the optimization and control of batch processes.

References

1. G. Oster and N. L. Yang, *Chem. Rev.*, **68**, 125 (1968).
2. C. Wallings and E. R. Briggs, *J. Am. Chem. Soc.*, **68**, 1141 (1946).
3. J. A. Biesenberger and D. H. Sebastian, *Principles of Polymerization Engineering*, Wiley-Interscience, New York, 1983.
4. J. N. Cardenas and K. F. O'Driscoll, *J. Polym. Sci., Polym. Chem. Ed.*, **14**, 883 (1976).
5. S. K. Soh and D. C. Sundberg, *J. Polym. Sci., Polym. Chem. Ed.*, **20**, 1331 (1982).
6. B. W. Brooks, *Proc. Roy. Soc. London A*, **357**, 183 (1977).
7. M. G. Kulkarni, R. A. Mashelkar, and L. K. Doraiswamy, *Chem. Eng. Sci.*, **35**, 823 (1980).
8. L. M. Arnett, *J. Am. Chem. Soc.*, **74**, 2027 (1952).
9. F. M. Lewis and M. S. Matheson, *J. Am. Chem. Soc.*, **71**, 747 (1949).
10. R. C. Petersen, J. H. Markgraff, and S. D. Ross, *J. Am. Chem. Soc.*, **83**, 3819 (1961).
11. H. Gerrens, in *Chemical Reaction Engineering*, Proc. of 4th Int/6th European Symp., Heidelberg, FRG, April 1976, Dechema, 1976.
12. F. L. Martin and A. E. Hamielec, *Am. Chem. Soc. Symp. Ser.*, **104**, 43 (1979).
13. S. T. Balke and A. E. Hamielec, *J. Appl. Polym. Sci.*, **17**, 905 (1973).
14. N. Friis and A. E. Hamielec, *Am. Chem. Soc. Symp. Ser.*, **24**, 82 (1976).
15. R. T. Ross and R. L. Laurence, *AIChE Symp. Ser.*, **72**, 74 (1977).
16. P. Hayden and Sir H. Melville, *J. Polym. Sci.*, **43**, 201 (1960).
17. T. J. Tulig and M. V. Tirrell, *Macromolecules*, **14**, 1501 (1981).
18. J. N. Cardenas and K. F. O'Driscoll, *J. Polym. Sci., Polym. Chem. Ed.*, **15**, 1883 (1977).
19. A. M. North and G. A. Reed, *Trans. Faraday Soc.*, **57**, 859 (1961).
20. S. W. Benson and A. M. North, *J. Am. Chem. Soc.*, **81**, 1339 (1959).
21. A. M. North, *Quart. Rev.*, **20**, 421 (1966).
22. J. C. Bevington, H. W. Melville, and R. P. Taylor, *J. Polym. Sci.*, **14**, 463 (1954).
23. P. J. Flory, *Principles of Polymer Chemistry*, Cornell Univ. Press, Ithaca, NY, 1953.
24. M. Morton and I. Piirma, *J. Am. Chem. Soc.*, **80**, 5596 (1958).
25. K. Ito, *J. Polym. Sci., Polym. Chem. Ed.*, **13**, 401 (1975).
26. S. Onogi, T. Kobayashi, Y. Kojima, and Y. Taniguchi, *J. Appl. Polym. Sci.*, **7**, 847 (1963).
27. C. F. Cornet, *Polymer*, **6**, 373 (1965).
28. D. T. Turner, *Macromolecules*, **10**(2), 221 (1977).
29. H. B. Lee and D. T. Turner, *Macromolecules*, **10**(2), 226 (1977).
30. H. B. Lee and D. T. Turner, *Macromolecules*, **10**(2), 231 (1977).
31. K. A. High, H. B. Lee, and D. T. Turner, *Macromolecules*, **12**, 332 (1979).
32. E. Abuin, E. Contreras, E. Gruttner, and E. A. Lissi, *J. Macromol. Sci. Chem.*, **A11**(1), 65 (1977).
33. E. Abuin and E. A. Lissi, *J. Macromol. Sci. Chem.*, **A11**(2), 287 (1977).
34. M. B. Lachinov, R. A. Simonian, T. G. Georgieva, and V. P. Zubov, *J. Polym. Sci., Polym. Chem. Ed.*, **17**, 613 (1979).

35. K. F. O'Driscoll, W. Wertz, and A. Husar, *J. Polym. Sci., Polym. Chem. Ed.*, **5**, 2159 (1967).
36. T. J. Tulig and M. V. Tirrell, *Macromolecules*, **15**, 459 (1982).
37. E. R. Robertson, *Trans. Faraday Soc.*, **52**, 426 (1955).
38. P. R. Dvornic and M. S. Jacovic, *Polym. Eng. Sci.*, **21**, 792 (1981).
39. E. Trommsdroff, H. Koelhe, and P. Lagally, *Macromol. Chem.*, **1**, 169 (1947).
40. R. G. W. Norrish and R. R. Smith, *Nature*, **150**, 336 (1942).
41. G. V. Schultz and G. Harborth, *Macromol. Chem.*, **1**, 106 (1947).
42. W. Y. Chiu, G. M. Carratt, and D. S. Soong, *Macromolecules*, **16**, 348 (1983).
43. A. V. Tobolsky and B. Baysal, *J. Polym. Sci.*, **11**, 471 (1953).
44. H. K. Mahabadi and K. F. O'Driscoll, *J. Macromol. Sci. Chem.*, **A11**(5), 967 (1977).
45. M. Stickler and G. Meyerhoff, *Macromol. Chem.*, **179**, 2729 (1978).
46. M. R. Gopalan and M. Santhappa, *J. Polym. Sci.*, **25**, 333 (1957).
47. J. Brandup and E. H. Immergut, Eds., *Polymer Handbook*, 2nd ed., Wiley-Interscience, New York, 1975.
48. P. E. Baillagou, M.S. thesis, University of California, Berkeley, 1983.
49. R. Jaisinghani and W. H. Ray, *Chem. Eng. Sci.*, **32**, 811 (1977).
50. R. H. Perry and C. H. Chilton, Eds., *Chemical Engineers' Handbook*, 5th ed., McGraw-Hill, New York, 1973.
51. R. C. Weast, Ed., *Handbook of Chemistry and Physics*, 62nd ed., CRC Press, Cleveland, OH, 1982.
52. B. M. Louie, M.S. thesis, University of California, Berkeley, 1984.
53. H. K. Mahabadi and K. F. O'Driscoll, *J. Polym. Sci., Polym. Chem. Ed.*, **15**, 283 (1977).
54. F. Bueche, *J. Chem. Phys.*, **20**, 1959 (1952).
55. H. Fujita, A. Kishimoto, and K. Matsumoto, *Trans. Faraday Soc.*, **56**, 424 (1960).
56. H. Fujita, *Fortschr. Hochpolym.-Forsch.*, **BD3**, S.1 (1961).
57. M. Doi and S. F. Edwards, *J. Chem. Soc. Faraday Trans. II*, **74**, 1789 (1978).
58. A. D. Schmidt and W. H. Ray, *Chem. Eng. Sci.*, **36**, 1401 (1981).
59. S. K. Soh and D. C. Sundberg, *J. Polym. Sci., Polym. Chem. Ed.*, **20**, 1345 (1982).
60. S. L. Liu and N. R. Amundson, *Rubber Chem. Technol.*, **34**, 995 (1961).
61. W. H. Ray, *J. Macromol. Sci., Rev. Macromol. Chem.*, **C8**(1), 1 (1972).
62. R. J. Zeman and N. R. Amundson, *AIChE J.*, **9**, 297 (1963).
63. S. Mimasu and T. Ayabe, *Polymerization Engineering*, Nikkan Kogyo Shinbun, Tokyo, Japan, 1967, p. 137.
64. D. J. Coyle, T. J. Tulig, and M. V. Tirrell, "Numerical Analysis of Polymerization Models Using The Finite Element Method," Paper 31d, AICHE Annual Meeting, Los Angeles, 1982.
65. W. Kuhn, *Chem. Ber.*, **63**, 1503 (1930).
66. G. V. Schultz, *Z. Phys. Chem. (Leipzig)*, **B30**, 379 (1935).
67. P. J. Flory, *J. Am. Chem. Soc.*, **59**, 241 (1937).
68. S. L. Rosen, *Fundamental Principles of Polymeric Materials*, Wiley-Interscience, New York, 1982.
69. C. H. Bamford and H. Tompa, *Trans. Faraday Soc.*, **50**, 1097 (1954).
70. A. M. Stolin, A. G. Merzhanov, and A. Y. Malkin, *Polym. Eng. Sci.*, **19**, 1065 (1979).
71. R. H. M. Simon and D. C. Chappelear, *Am. Chem. Soc. Symp. Ser.*, **104**, 71 (1979).
72. F. S. Dainton and K. J. Ivin, *Quart. Rev.*, **12**, 61 (1958).
73. J. A. Biesenberger and R. Capinpin, *Polym. Eng. Sci.*, **14**, 737 (1974).
74. A. V. Tobolsky, *J. Am. Chem. Soc.*, **80**, 5927 (1958).
75. D. H. Sebastian and J. A. Biesenberger, *Polym. Eng. Sci.*, **16**, 117 (1976).
76. J. A. Biesenberger, R. Capinpin, and Y. C. Yang, *Polym. Eng. Sci.*, **16**, 101 (1976).

Received September 20, 1984
Accepted February 1, 1985